The 20th Cambridge Workshop on Cool Stars, Stellar Systems, and the Sun
Edited by S. J. Wolk

The Solar Wind in Time II: can we detect radio emission from young solar analogues?

Dúalta Ó Fionnagáin[1], Aline A. Vidotto[1], Pascal Petit[2,3], Colin P. Folsom[2,3], Sandra V. Jeffers[4], Stephen C. Marsden[5], Julien Morin[6], and José-Dias do Nascimento Jr.[7,8]

[1]School of Physics, Trinity College Dublin, College Green, Dublin 2, Ireland
[2]Université de Toulouse, UPS-OMP, Institut de Recherche en Astrophysique et Planétologie, Toulouse, France
[3]IRAP, Université de Toulouse, CNRS, UPS, CNES, 31400, Toulouse, France
[4]Universität Göttingen, Institut für Astrophysik, Friedrich-Hund-Platz 1, 37077 Göttingen, Germany
[5]University of Southern Queensland, Centre for Astrophysics, Toowoomba, QLD, 4350, Australia
[6]Laboratoire Univers et Particules de Montpellier, Université de Montpellier, CNRS, F-34095, France
[7]Dep. de Física, Universidade Federal do Rio Grande do Norte, CEP: 59072-970 Natal, RN, Brazil
[8]Harvard-Smithsonian Center for Astrophysics, Cambridge, MA 02138, USA

Abstract

The solar wind in the preset is well studied using remote and in situ measurements. Not much is known about the evolution of the solar wind over the lifetime of our star, posing the question, what was the solar wind like over evolutionary timescales? To answer this question we turn to solar-like stars that we can use as proxies for the solar wind at different ages. There currently exists little information on the winds of solar-like stars as observations are difficult to conduct due to their rarefied nature which leads to diminished emissions. We present 3D MHD simulations of a sample of solar analogues from which we determine global wind parameters such as mass- and angular momentum-loss rates. From our simulations we calculated the thermal bremsstrahlung expected from these winds using a developed numerical tool, comparing them to the sensitivities of current and future radio telescopes.

1 Introduction

Stellar winds are the mechanism by which stars lose angular-momentum and spin down (Weber & Davis, 1967). This can have a significant effect on regulating stellar activity with rapidly rotating stars displaying higher levels of stellar activity than slowly rotating stars (Wright *et al.*, 2013). High activity levels might have consequences for the development of habitable planets orbiting these stars (e.g. Chadney *et al.* 2017). Intense radiation from a host star can expedite evaporation of planetary atmospheres and can act as an indirect biocide (Ribas *et al.*, 2005). Active stars also have more intense magnetic fields (Folsom *et al.*, 2018), which affect acceleration and propagation of stellar winds (Washimi & Shibata, 1993).

To investigate the evolution of the solar wind we simulate the winds of solar analogues at different ages and rotation rates, using them as proxies for the solar wind at different points in its evolution. We develop a code to calculate the thermal bremsstrahlung emitted from the winds of these stars, as this information (and possible detections/upper-limits) can give insight into global features of the star, such as mass-loss rate (Panagia & Felli, 1975; Vidotto & Donati, 2017; Fichtinger *et al.*, 2017). Details of this work can be found at Ó Fionnagáin *et al.* (2018).

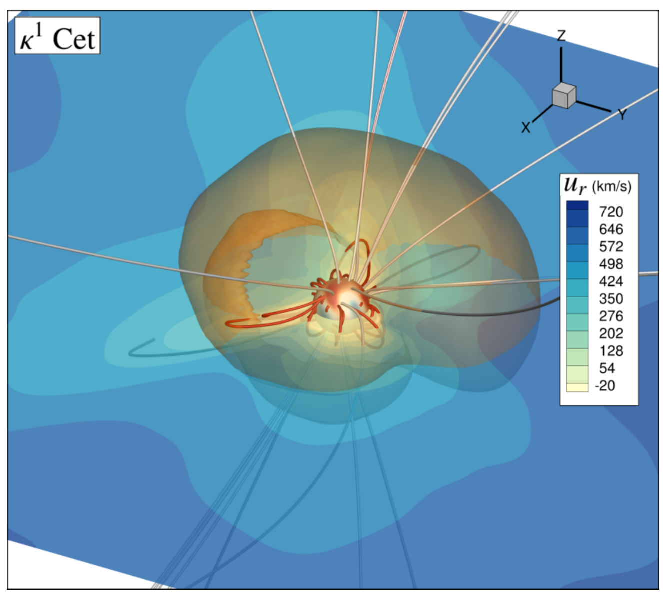

Figure 1: 3D MHD simulation of the stellar wind of κ^1 Ceti.

2 3D wind simulations

We solve the ideal MHD equations for the stellar wind using the BATS-R-US numerical modelling tool (Powell *et al.*, 1999). Free parameters that are required from our models are: base wind density, base wind temperature and a polytropic index. We adopt the scaling laws presented in Ó Fionnagáin & Vidotto (2018). The stellar magnetic field is required by the simulation as an input. We use surface stellar magnetic fields observationally derived with the Zeeman-Doppler Imaging technique (Donati & Semel, 1990). The observed magnetic fields used in our study are from Petit *et al.* (2008); do Nascimento *et al.* (2016) and Petit, *et al.* (in prep.).

An example output of the simulation is shown in Figure 1 for κ^1 Ceti. Shown in the z=0 plane is the wind velocity, ranging from -20—720 km s^{-1}. The orange surface represents the Alfvén surface where the wind velocity equals the Alfvén velocity ($u_r = v_A = B/\sqrt{4\pi\rho}$). Regions within this surface are magnetically dominated. Closed magnetic (B) field lines are shown in red and open field lines in grey.

From these simulations we calculate the mass-loss rate, angular momentum-loss rate, and open flux associated with each star (Figure 2). We see an overall decrease in all three of these parameters as the stars spin down, showing that slowly spinning stars lose less mass and angular-momentum than their rapidly spinning counterparts. Figure 2 (*top*) shows a fit to the mass-loss rates of stars rotating faster than 1.4 $\Omega_\odot$ (solid red line), which presents a similar fit to fast solar-type rotators from Ó Fionnagáin & Vidotto (2018) (solid black line).

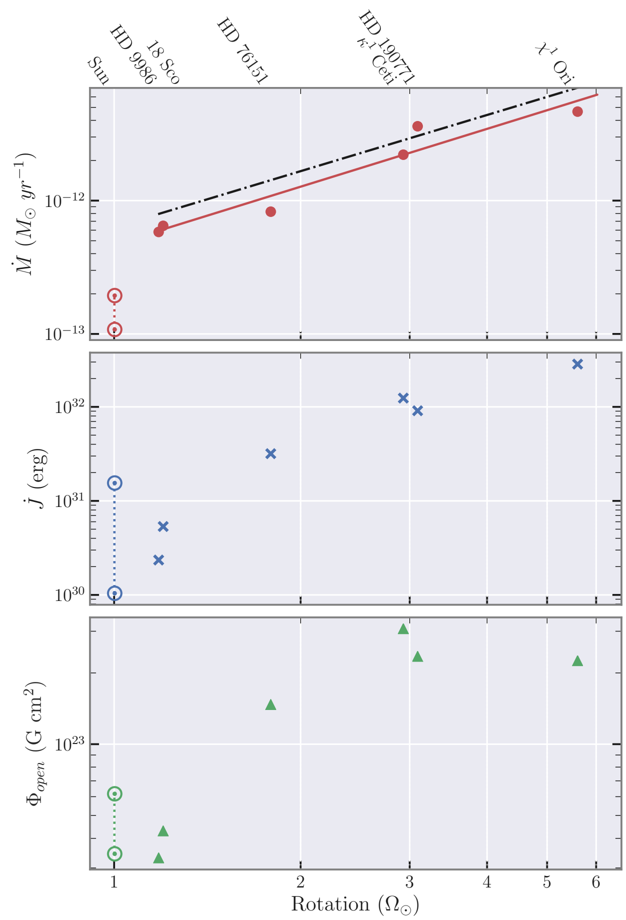

Figure 2: Top to bottom: mass-loss rate, angular momentum-loss rate, and unsigned magnetic open flux from our sample of simulations. The stars are labelled at the top of the figure, with the solar simulations represented by the solar symbol (⊙), where activity maximum is always on top. In the top panel we include a fit to the data (red line, excluding the Sun) and compare this to the fast rotator fit as described in Ó Fionnagáin & Vidotto (2018) (black dashed line).

3 Radio Emission

We developed a code for numerically solving the radiative transfer equation for thermal emission from our simulation grid (Ó Fionnagáin, 2018). The plasma around a star will emit thermally in the radio in accordance with the radiative transfer equation:

$$I_\nu = \int_{-\infty}^{\tau'_{\max}} B_\nu e^{-\tau} d\tau' \quad (1)$$

Where I$_\nu$ is the specific intensity of emission, τ is the optical depth (which depends on density squared), and B$_\nu$ is the blackbody function. Previous calculations of thermal radio emission from winds have made analytical assumptions about the density distribution in the wind (Panagia & Felli, 1975; Reynolds, 1986; Fichtinger *et al.*, 2017; Vidotto & Donati, 2017). By solving the radiative transfer equation we remove any assumption of density distribution in the wind. We solve Equation (1) for frequencies ranging from 100 MHz to 100 GHz and present these spectra in Figure 3. In Figure 3, we show the sensitivity levels of the current VLA (green), SKA1-MID (red), and SKA2-MID (blue), along with observations of direct detections of χ^1 Ori (purple stars) and upper limits of κ^1 Ceti as observed by Fichtinger *et al.* (2017). Current instrumentation is not sensitive enough to detect these tenuous winds, but instruments such as ngVLA, SKA1 and SKA2 present opportunity to detect these winds in the future.

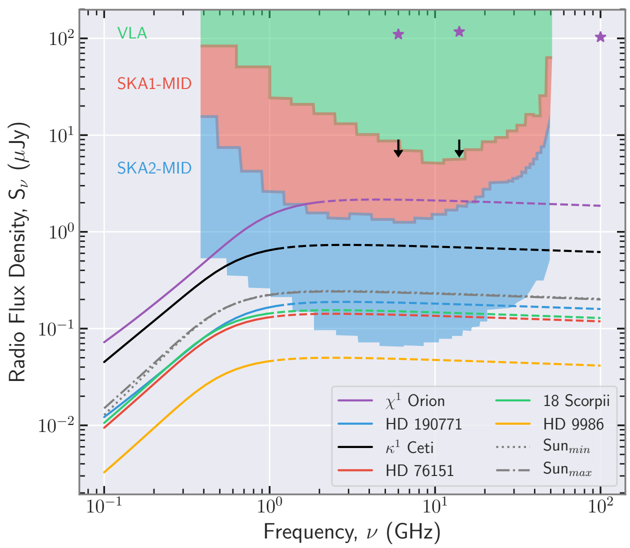

Figure 3: Calculated spectra for each star. While out of reach of current instrumentation, we predict that detecting these winds through thermal radio could become a possibility with the advent of SKA1 and SKA2 in particular. SKA sensitivities from Pope *et al.* (2018) and adjusted for 2 hour integration time.

4 Can we detect radio emission from the young solar wind?

Detection of solar-type stellar winds in the radio regime is challenging. There have been previous attempts to do so (Gaidos *et al.*, 2000; Villadsen *et al.*, 2014; Fichtinger *et al.*, 2017), yet to no avail. However, upper-limits of wind density can be derived from non-detections in thermal radio emission, from which stellar mass-loss constraints can be calculated. Even within the optically thin regions of the wind, if chromospheric emission of flares can be detected, this will still place useful constraints on the wind density as the wind must be optically thin at the observing frequency if these phenomena are observed (Reynolds, 1986). Disentangling the chromospheric emission from the wind emission can be difficult, but can be deduced from the level of emission detected. Villadsen *et al.* (2014) and Fichtinger *et al.* (2017) detected chromospheric emission from multiple solar analogues, which emitted at the ≈ 100 μJy level. Since we expect the wind emission to exist two orders of magnitude less than this we can deduce that their detections were indeed chromospheric emission. Observations in the optically thick region are preferable but more difficult as the flux density decreases in these regions according to the spectra in Figure 3, due to the density falling off in the higher stellar atmosphere. Despite this, we predict that some of the closer solar analogue winds should be detectable in the optically thick regime with future instrumentation, such as SKA2-MID and possibly SKA1-MID.

Acknowledgements

DÓF gratefully acknowledges financial support to attend CS20 from the Trinity Travel Trust Grant and partially from the IRC Laureate Award. DÓF would like to acknowledge research funding through the Trinity Postgraduate Award. AAV acknowledges funding from the Irish Research Council Laureate Awards 2017/2018. The authors wish to acknowledge the DJEI/DES/SFI/HEA Irish Centre for High-End Computing (ICHEC) for the provision of computational facilities and support. This work used the BATS-R-US tools developed at the University of Michigan Center for Space Environment Modeling and made available through the NASA Community Coordinated Modeling Center.

References

Ó Fionnagáin, D., Vidotto, A. A., Petit, P., Folsom, C. P., Jeffers, S. V., *et al.* 2018, ArXiv e-prints, arXiv:1811.05356.
Chadney, J. M., Koskinen, T. T., Galand, M., Unruh, Y. C., & Sanz-Forcada, J. 2017, A&A, 608, A75.
do Nascimento, J., J. D., Vidotto, A. A., Petit, P., Folsom, C., Castro, M., *et al.* 2016, ApJ, 820, L15.
Donati, J. F. & Semel, M. 1990, SoPh, 128, 227.
Fichtinger, B., Güdel, M., Mutel, R. L., Hallinan, G., Gaidos, E., *et al.* 2017, A&A, 599, A127.
Folsom, C. P., Bouvier, J., Petit, P., Lèbre, A., Amard, L., *et al.* 2018, MNRAS, 474, 4956.
Gaidos, E. J., Güdel, M., & Blake, G. A. 2000, Geophysical Research Letters, 27, 501.
Ó Fionnagáin, D. 2018, *ofionnad/radiowinds: Calculating Thermal Bremsstrahlung Emission from Stellar Winds.*
Ó Fionnagáin, D. & Vidotto, A. A. 2018, MNRAS, 476, 2465. ISSN 0035-8711.
Panagia, N. & Felli, M. 1975, A&A, 39, 1.
Petit, P., Dintrans, B., Solanki, S. K., Donati, J. F., Aurière, M., *et al.* 2008, MNRAS, 388, 80.
Pope, B. J. S., Withers, P., Callingham, J. R., & Vogt, M. F. 2018, ArXiv e-prints, arXiv:1810.11493.
Powell, K. G., Roe, P. L., Linde, T. J., Gombosi, T. I., & De Zeeuw, D. L. 1999, J. Comp. Phys., 154, 284. ISSN 00219991.
Reynolds, S. P. 1986, ApJ, 304, 713.
Ribas, I., Guinan, E. F., Güdel, M., & Audard, M. 2005, ApJ, 622, 680.
Vidotto, A. A. & Donati, J. F. 2017, A&A, 602, A39.
Villadsen, J., Hallinan, G., Bourke, S., Güdel, M., & Rupen, M. 2014, ApJ, 788, 112.
Washimi, H. & Shibata, S. 1993, MNRAS, 262, 936.
Weber, E. J. & Davis, J., Leverett 1967, ApJ, 148, 217.
Wright, N. J., Drake, J. J., Mamajek, E. E., & Henry, G. W. 2013, Astronomische Nachrichten, 334, 151.